Methanol Synthesis Catalysis in an Internally Recycled Reactor

C. E. BROWN and C. O. BENNETT

The University of Connecticut, Storrs, Connecticut

A gradientless reactor has been tested by measurement of the chemical reaction rate in the synthesis of methanol from carbon monoxide and hydrogen. The reactor behaves as a well-stirred tank, and data have been obtained at 3,000 lb./sq.in.abs. over the temperature range 300° to 400°C.

Rate data have been obtained for commercial zinc chromite catalyst in particle form and for the commercial ¼-in. pellets. The effectiveness factors derived from these experiments have been used to estimate the tortuosity of the pellets; it is found to agree qualitatively with the value measured from experiments on pure diffusion in a catalyst pellet.

The work reported here offers two main results. First, a versatile gradientless reactor has been tested and should prove useful for a variety of laboratory studies. Second, effectiveness factors for the methanol synthesis reaction

$$CO + 2H_2 \rightleftarrows CH_3OH$$

have been measured at 207 bars (3,000 lb./sq.in.abs.) for the well-defined temperatures and compositions which can be obtained in the laboratory reactor. Commercial zinc chromite catalyst has been used in sizes from 6.3 to 0.4-mm. particles.

THE KINETICS OF METHANOL SYNTHESIS

The first reported extensive laboratory study of the kinetics of the methanol synthesis was performed by Natta and his associates. The review by Natta (*1*) summarizes this work and surveys previous literature on the subject. Several different catalysts containing ZnO were used in the form of 0.6- to 0.9-mm. particles. An integral, isothermal reactor was operated in the pressure range 200 to 300 bars and the temperature range 300° to 400°C. The results were well represented by a Langmuir-Hinshelwood scheme; surface reaction was reported as the controlling step. The constants in Natta's correlating equation were later determined by nonlinear estimation (*2*).

A few years later Uchida and his associates reported a series of studies on the reaction catalyzed by zinc oxide-chromic oxide mixtures at 300° to 400°C. and 200 to 300 bars. Laboratory studies were made with an integral reactor containing about 5 cc. of catalyst of 2 to 3 mm. size (*3* to *6*). In 1962 further studies were made (*7, 8*) in a larger reactor containing 1.74 liters of 3- to 4-mm. catalyst pellets. Concentration and temperature traverses were made in the catalyst beds both with and without heat removal. The laboratory rate data were explained by an equation of the Temkin-Pyshev type (*9*), with the desorption of methanol as the controlling step. The adsorption of carbon monoxide on methanol synthesis catalyst has also been studied (*10*).

Vlasenko, Rozenfel'd, and Rusov (*11*) studied the reaction at 300° to 400°C. and 200 to 300 bars in a 32-mm. diameter catalyst tube which was part of a small pilot plant. Catalyst particles of 0.5 to 1 and 4 to 5 mm. sizes were used. The activity of the smaller catalyst particles was higher, but no effectiveness factors were calculated. Münzing (*12*) has reported tests on a number of different catalyst compositions, including those used by the Uchida and by the Natta groups. A commercial Leuna catalyst proved to be at least as active as any of the other modifications studied.

A useful review of the methods and data available for designing a methanol synthesis converter has been written by Vachez and Leprince (*13*); the work is based on the results of Natta (*1*). Heat and mass transfer effects for the commercial zinc oxide-chromic oxide synthesis catalyst have been calculated by Pasquon and Dente (*14*). They found that operating effectiveness factors of 0.5 to 0.7 were to be expected, in accord with some data on commercial reactors.

Catalysts containing copper have been studied from time to time (*1*). They are more active than the zinc chromite catalysts but have apparently not been used commercially because of their susceptibility to sulfur poisoning. However, improvements in the purity of commercially feasible synthesis gas have led to a revival of interest in such catalysts. They permit operation at lower temperature and pressure than the standard type and thus provide economies in capital and operating costs (*15*).

THE INTERNALLY RECYCLING REACTOR

All the studies so far discussed have been made in integral reactors. Although such reactors can be made approximately isothermal, concentration gradients cannot be eliminated. Rates of reaction must be obtained from the experimental results by the inherently inaccurate process of differentiating the data. The ordinary differential reactor suffers from the difficulty of obtaining accurate rate data from the small difference between the inlet and outlet compositions. These considerations have led to the popularity of the recycling reactor. These matters have been considered by Carberry, and he has proposed (*16*) and later used (*17*) a continuous stirred tank catalytic reactor. This type of reactor appears to be more adaptable to operation at high pressure than the more common gradientless reactor with external recirculation ducts and pumps. In addition, the recycled gas need not be cooled and heated in the internally recycled (stirred tank) reactor.

An interesting discussion of the design of laboratory reactors is given by Brisk, Day, Jones, and Warren (*18*). These authors have designed and tested a stirred reactor with less void space than Carberry's reactor (*17*). An internally recycled reactor suitable for high-pressure studies has been designed by Garanin, Kurkchi, and Minachev (*19*). This design seems superior to other stirred reactors already proposed by a number of other Russian investigators (*20* to *23*).

The importance of a temperature difference between the bulk of the gas and the catalyst surface has recently

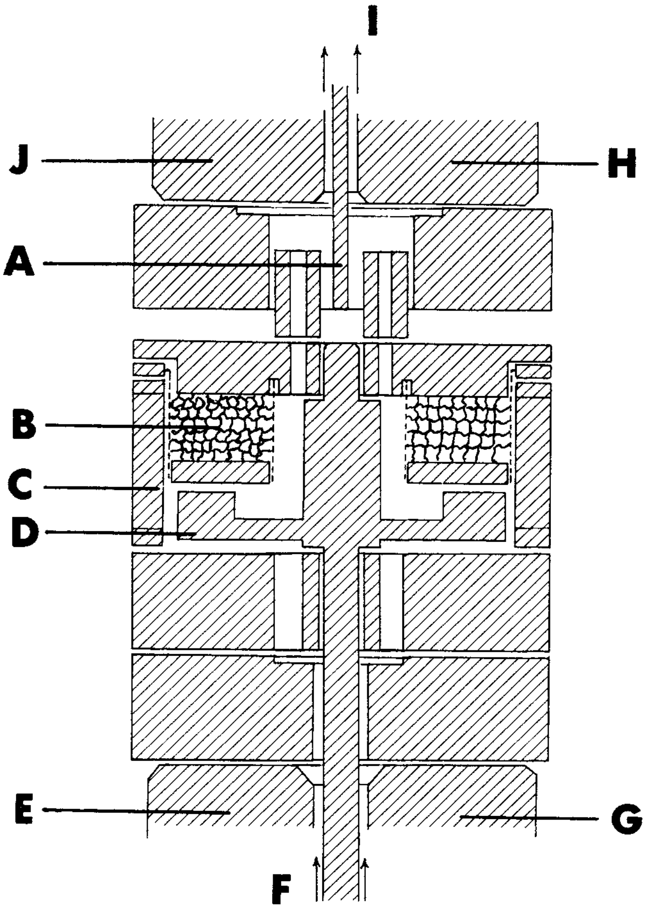

Fig. 1. Internally recycling reactor internals: A. thermocouple, B. catalyst in annular basket, C. baffle, D. turbine, E. lower closure, F. gas inlet, I. gas outlet, J. upper closure.

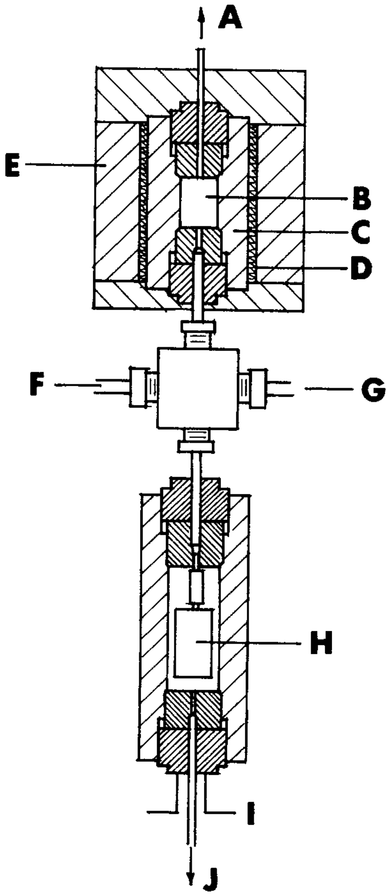

Fig. 2. Two-chamber high-pressure reactor: A. exit gas, B. reaction chamber, C. reactor shell, D. electric band heater, E. insulation, F. inlet gas, G. blowout disk, H. turbine motor, I. electrical leads, J. gas bleed.

been emphasized (*24* to *26*). Chambers and Boudart (*27*) have pointed out that such interphase resistances are common in laboratory differential or integral reactors, which often operate at a low Reynolds number. A distinct advantage of a recycling reactor is that the gas velocity past the catalyst surface can be increased to the limit of the circulating device without changing the residence time.

In the continuous stirred tank catalytic reactor (*17, 18*) the catalyst particles are confined to baskets which are rotated through the reacting gas. For small particles, it seems probable that the baskets may act as turbine blades, so that the gas flows mainly outward radially and may not be forced through the particles in the basket. Partly for this reason, Carberry had proposed to coat fine particles on spheres held in the basket. The reactor used in the present work, shown in Figure 1, is so arranged that the recycling gas is forced to flow radially inward through a bed of catalyst particles. The gas is thrown outward by a turbine and then directed up around the outside of the annular catalyst basket by vertical baffles. It then flows inward through the catalyst bed to be drawn into the turbine once more.

The reactor body is made of A286 steel and is designed for operation at 1,000 bars and 500°C. The turbine motor is housed in the lower vessel (at room temperature) shown in Figure 2, and the drive shaft for the turbine extends up through the high-pressure tubing which connects the two vessels. The reactor feed enters through the tube containing the drive shaft, and a small bleed of gas through the motor enclosure is provided to prevent vapors from the motor from coming into contact with the catalyst. The equipment flow sheet is shown in Figure 3.

THE MEASUREMENT OF EFFECTIVENESS FACTORS

There is a rather extensive literature on analytical or numerical solutions of the conservation equations for various chemical kinetics rate expressions to give the effectiveness factor of a catalyst pellet as a function of the Thiele modulus and other parameters (*28*). Satterfield and Sherwood (*28*) also give a table of results for experi-

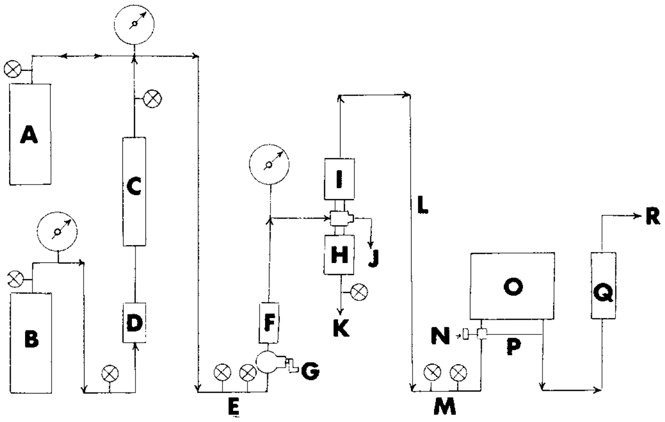

Fig. 3. Equipment flow sheet: A. high-pressure storage vessel, B. low-pressure storage vessel, C. diaphragm compressor, D. filter, E. valves, F. guard adsorbants. G. pressure controller, H. motor vessel, I. reactor, J. blowout line, K. bleed line, L. reactor outlet line, M. needle valves, N. sample valve, O. chromotograph, P. bypass line, Q. flow measurement, R. effluent to hood.

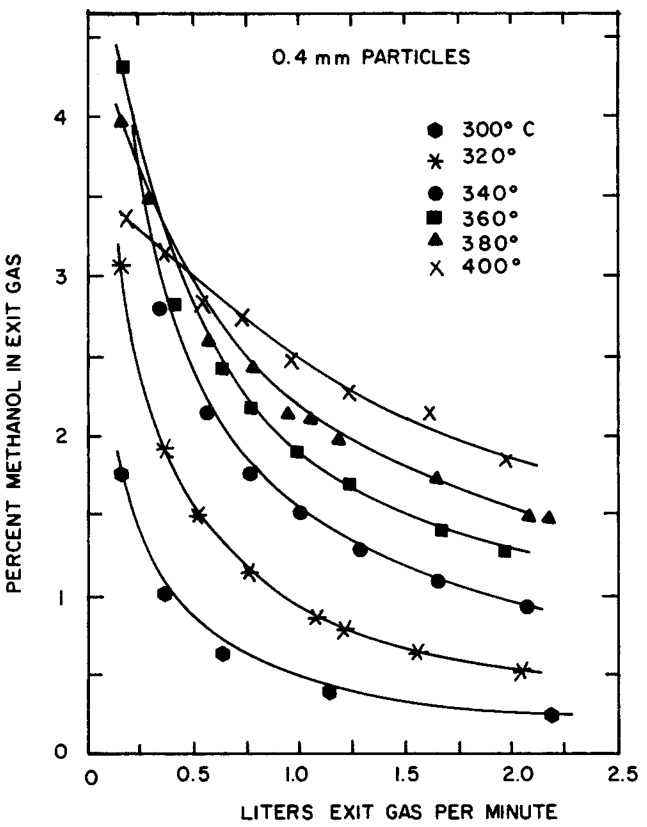

Fig. 4. Experimental results for 0.254 g. of 0.4-mm. particles. Reaction pressure, 207 bars; exit gas condition at flow measurement, 750 mm. Hg and 21°C.

mental studies of the effectiveness factor, and these papers are not so numerous. Most such studies are based on the measurement of the activities of catalyst particles of differing sizes. More recent studies, all of which employ this method, are listed in the bibliography (*29* to *35*).

An interesting way to investigate effectiveness factors for reactions with a strong heat effect is to measure the temperature distribution inside a catalyst pellet during reaction. This method has been successfully employed by several workers (*36 to 38*).

EXPERIMENTAL RESULTS

A commercial catalyst, (Harshaw Zn-0312-T-¼) ¼-in. diameter by ¼-in. height, was used in the experiments. The catalyst specifications are as follows: zinc oxide, 73%; chromic oxide, 21%; chromic acid, 0.01%; carbon, 0.8%; density, 2.50 g./cc.; crushing strength, 36 lb.; surface area, 130 sq. m./g.; porosity, 0.500; pore size distribution, in terms of cumulative pore volume, cc./gram: Up to 180 Å, 0.11; to 200 Å, 0.12; to 300 Å, 0.14; to 700 Å, 0.16; to 1000 Å, 0.18; to 10,000 Å, 0.19; and to 150,000 Å, 0.20 (pore volume, 0.20 cc./g.).

The results of the kinetic studies at 207 bars for the temperature range 300° to 400°C. are shown in Figure 4 for the 0.4-mm. particles (prepared by crushing the commercial pellets) and in Figure 5 for the 6.3-mm. pellets.

The feed gas composition was 10.8 mole % carbon monoxide, remainder hydrogen, for all work reported here. This composition was chosen to enhance the reaction rate and to avoid any side reactions (*1*). Chromatographic analyses (flame ionization detector) of the reactor effluent for all work always showed the presence of no organic products other than methanol.

Interphase heat and mass transfer resistances were in-

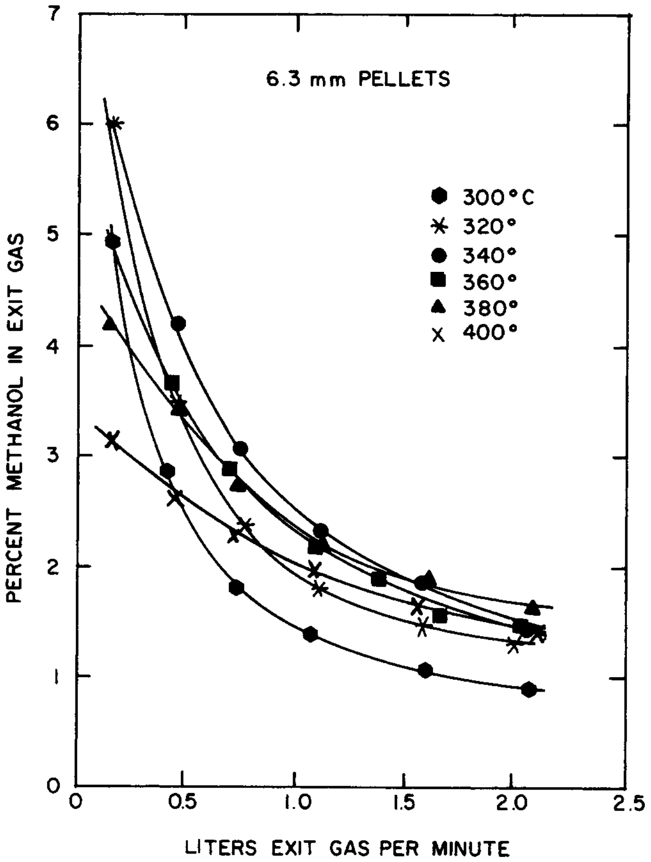

Fig. 5. Experimental results for 1.087 g. of 6.3-mm-pellets. Reaction pressure, 207 bars; exit gas condition at flow measurement, 750 mm. Hg and 21°C.

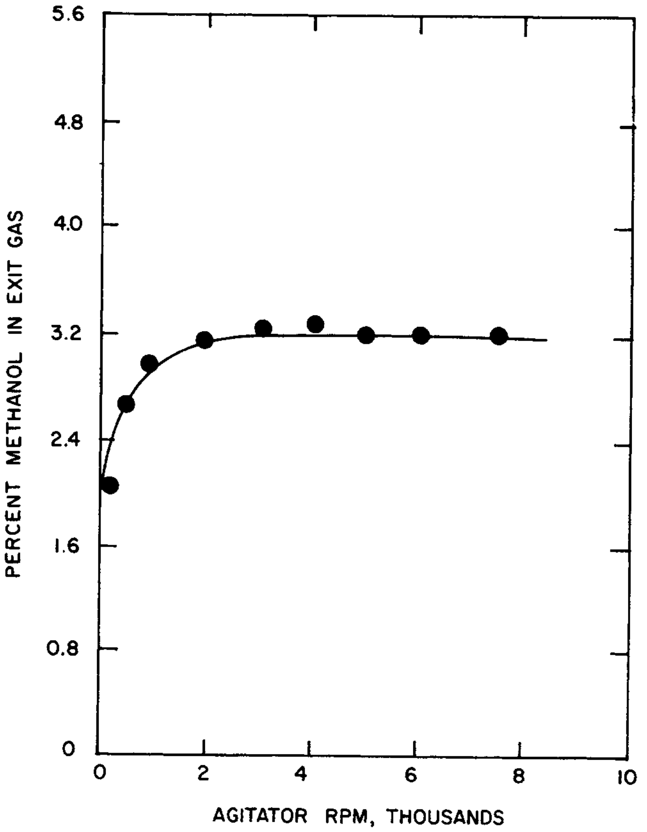

Fig. 6. Test for mass and heat transfer effects. 380°C. and 207 bars for the 0.4-mm. catalyst. Flow rate, 442 ml./min. at 753 mm. Hg and 27°C.

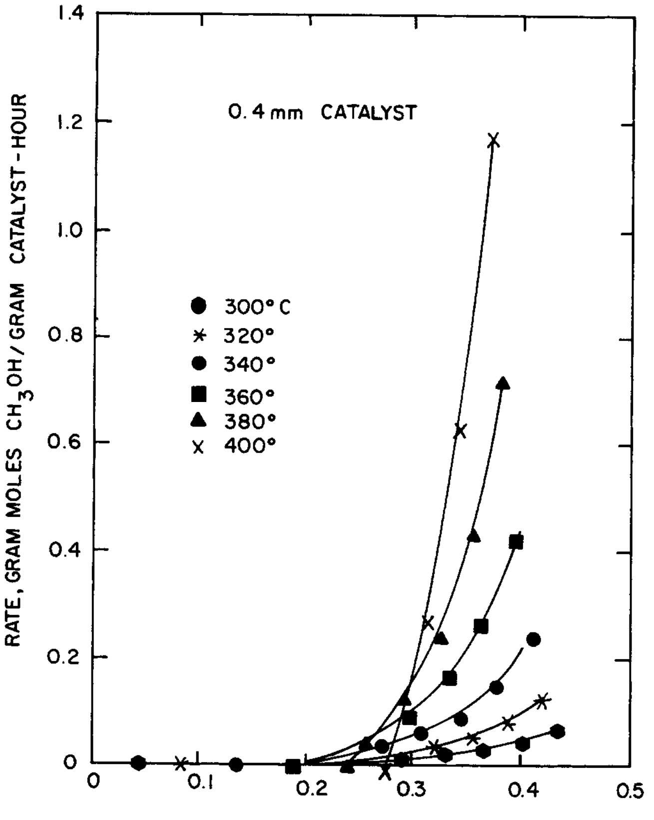

Fig. 7. Rates of reaction for the 0.4-mm. catalyst at 207 bars.

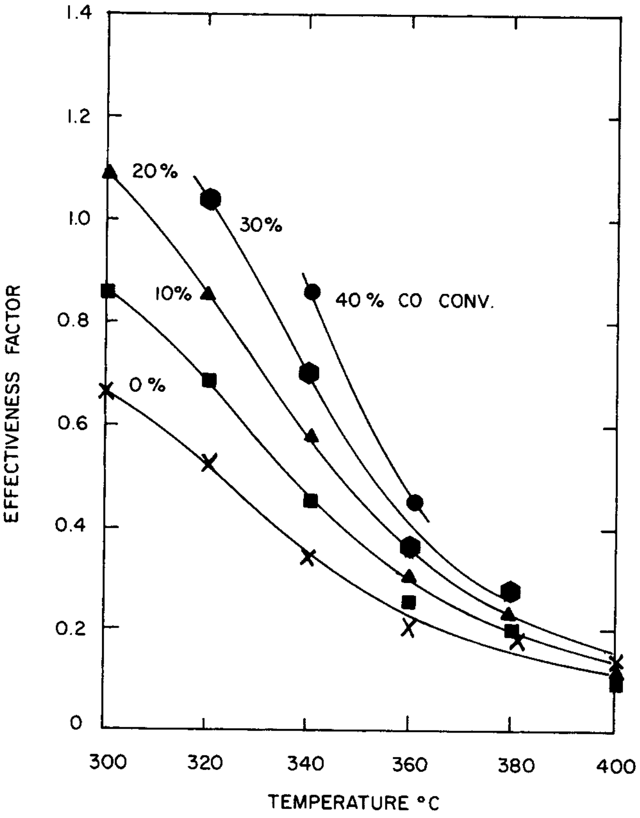

Fig. 9. Effectiveness factors for the 6.3-mm. pellets at 207 bars.

vestigated by varying the speed of the turbine for the 0.4-mm. catalyst for conditions corresponding to a relatively high reaction rate. The results, shown in Figure 6, give evidence that interphase resistance is not important for turbine speeds above 2,000 rev./min.

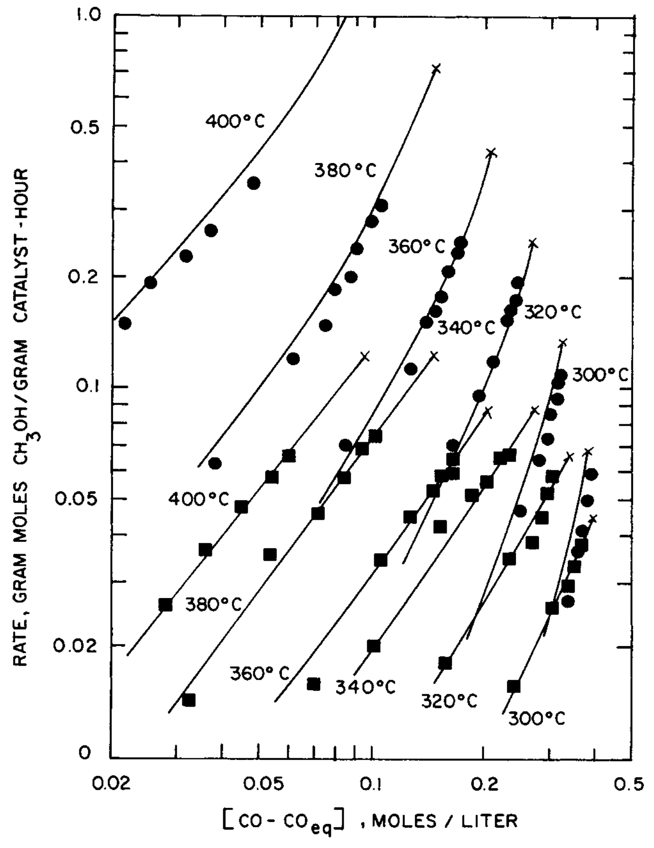

Fig. 8. Rates of reaction for particles (⊙) and pellets (□) at 207 bars.

This method of evaluation appears more reliable than the calculation of the mass transfer coefficient based on an estimation of the circulation rate caused by the turbine. A speed of 3,000 rev./min. or more was used for the rest of the work reported here.

Intraphase mass and heat transfer effects were investigated in a preliminary series of experiments on catalyst of 3.1, 1.55, 0.8, and 0.4 mm. nominal sizes at 380°C. and 207 bars. The reaction rates obtained at given concentrations increased with decreasing particle size until the 0.8 mm. size; this size gave results identical to those for the 0.4 mm. size, within experimental scatter. These data (*39*) indicate that it is correct to calculate the effectiveness factors for the 6.3-mm. pellets as the ratio of the rate over these pellets divided by the rate over the 0.4-mm. particles for a given bulk temperature and composition.

The amount of catalyst used (0.254 g. of 0.4-mm. particles, 1.087 g. of 6.3-mm. pellets) was chosen to give convenient gas flow rates. This quantity was not sufficient to fill the catalyst basket, so the remainder of the basket was always filled with glass beads of the same nominal size as the catalyst particles. Blank runs show no conversion to methanol in the absence of the catalyst.

The data of Figure 6 show also that the recycled reactor can be treated as a continuous stirred tank reactor. The rate of formation of methanol is thus easily calculated as the product of the molar concentration and volumetric flow rate of the reactor effluent.

Rate data for the 0.4-mm. particles are shown in Figure 7. The compositions shown for zero rate correspond to the calculated chemical equilibrium.

For the calculation of the effectiveness factors it is convenient to have algebraic rate expressions for both catalyst sizes. For the fine particles, the expression of Natta (*1*)has been used:

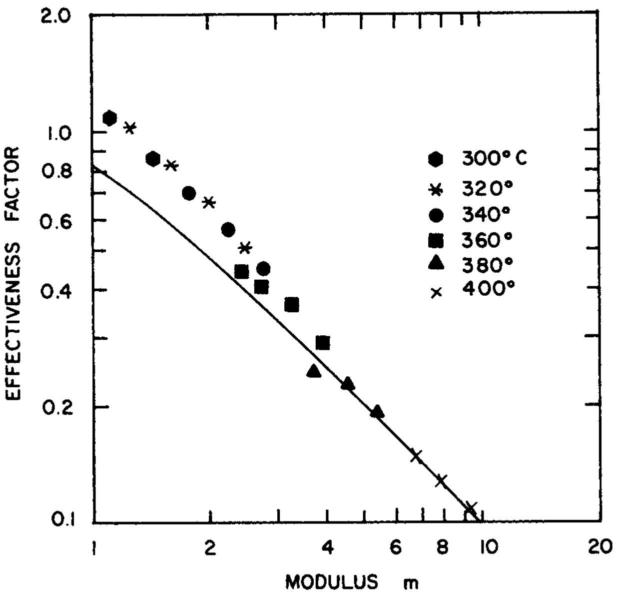

Fig. 10. Correlation of effectiveness factors for the 6.3-mm. pellets at 207 bars. The solid line is calculated from the data for the 0.4-mm. particles by the method of Bischoff (*48*). A value of 7.2 was used for τ.

$$r = \frac{f_c f_h^2 - f_m/K}{(A + Bf_c + Cf_h + Df_m)^3} \qquad (1)$$

Fugacities have been retained in this equation as used by Natta (1), although transition state theory would lead to the use of concentrations (*40, 41*).

The details of the evaluation of the constants in this equation are given elsewhere (*39*). For this work, added data at a different feed composition and at different total pressures were obtained (*39*). The values of the constants and their behavior with temperature are similar to those found by Natta (1). The present catalyst is about four times more active than his.

For the 6.3 mm. rate data, it was observed that a log-log plot of rate against $c - c_{eq}$ was a straight line, within experimental precision. Figure 8 gives the results of all the pertinent rate data for the two catalyst sizes. The solid lines represent Equation (1) for the fine particles, and an equation of the form

$$r = k\,(c - c_{eq})^n \qquad (2)$$

was used for the pellets. For a given concentration and temperature, the effectiveness factor is simply the ratio of the rates obtained from these two equations. Figure 9 gives the effectiveness factors calculated in this way. The expected decrease in effectiveness factor with increased reaction rates is confirmed by this graph.

ESTIMATION OF PELLET TORTUOSITY

At 207 bars the mean free path is small enough to ensure the predominance of ordinary molecular diffusion in all but the smallest pores. In the absence of Knudsen diffusion, it is sufficient to characterize the porous nature of the catalyst pellet by the simple equation for the effective diffusivity (*28*):

$$D_{\text{eff}} = \frac{D_c\,\epsilon}{\tau} \qquad (3)$$

From the Stefan-Maxwell equation (*42*) and the fluxes of the three gaseous components imposed by the stoichiometry of the reaction, there results

$$\frac{1}{D_c} = \frac{1}{D_{\text{CO-H}_2}}(x_h - 2x_c) + \frac{1}{D_{\text{CO-M}}}(x_m + x_c) \qquad (4)$$

From Equation (4) D_c can be calculated as a function of concentration at a given pressure and temperature. The variation is not negligible; for instance, at 380°C. and 207 bars, for zero carbon monoxide conversion D_c is 12.36×10^{-3} sq.cm./sec., and at 20% carbon monoxide conversion it is 11.80×10^{-3} sq.cm./sec. (*39*).

The binary diffusivities D_{ij} have been calculated by the correlation of Fuller, Schettler, and Giddings (*43*), which indicates that D_{ij} is proportional to $T^{1.75}$ and inversely proportional to pressure. Some work has been done on the measurement (*44*) and prediction (*45* to *47*) of diffusion at high pressure, but the effect of pressure cannot yet be estimated reliably. For a mixture rich in hydrogen, the method of Slattery and Bird (*45*) seems to predict very little reduction in the $p\,D_{ij}$ product. In the present work $p\,D_{ij}$ has merely been assumed constant.

For the concentration-dependent diffusivity and the complicated rate expression of Equation (1) it is convenient to use the method of Bischoff (*48*) for the calculation of the effectiveness factor. A modulus is defined as

$$m = \frac{D_0\,r_0}{6\sqrt{2}}\left[\int_{c_{eq}}^{c_0} D_{\text{eff}}(\alpha)\,r(\alpha)\,d\alpha\right]^{-1/2} \qquad (5)$$

This modulus is defined (*48*) so that it behaves like the modulus defined by Aris (*49*); that is, η equals $1/m$ for m greater than about 3. The effectiveness factor itself is calculated by

$$\eta = \frac{6\sqrt{2}}{D_0\,r_0}\left[\int_{c_L}^{c_0} D_{\text{eff}}(\alpha)\,r(\alpha)\,d\alpha\right]^{1/2} \qquad (6)$$

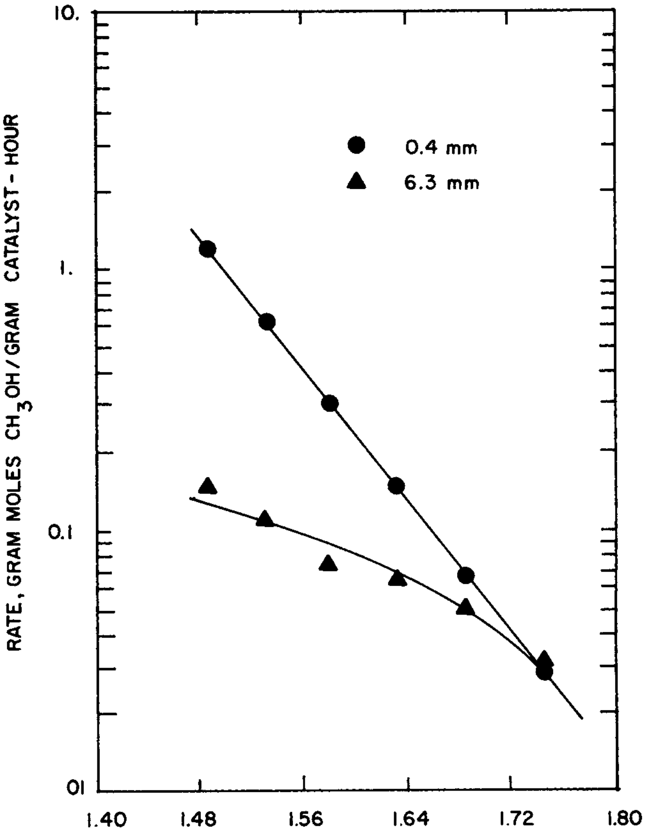

Fig. 11. Arrhenius plot of the measured rates at 207 bars and a carbon monoxide concentration of 0.373 g. moles/liter.

The quantity c_L is found implicitly from the equation

$$D_0 = \frac{6}{\sqrt{2}} \int_{c_L}^{c_0} D_{\text{eff}}(\beta) \left[\int_{c_L}^{\beta} D_{\text{eff}}(\alpha)\, r(\alpha)\, d\alpha \right]^{-1/2} d\beta \qquad (7)$$

In Equations (5) through (7), α and β are dummy variables representing the concentration of carbon monoxide.

From the above relations we can now estimate the tortuosity τ by trial. Once a value of τ is assumed, $D_{\text{eff}}(c)$ can be obtained and the modulus m calculated. Then a series of c_L ($c_L > c_{\text{eq}}$) are tested by Equation (7) until it is satisfied; η is finally calculated from the appropriate c_L. The correct value of τ is that which gives the calculated curve of η vs. m which most nearly represents the measured values of η when plotted against m. An IBM-360 digital computer system was used for the calculations.

In the above way a value of 7.2 for the tortuosity has been obtained; Figure 10 shows the appropriate plot of η vs. m. Since the points do not follow the calculated line exactly, the most weight has been given to the high modulus region, where diffusion effects predominate. In the region of low η, the experimental line also has a slope that agrees with theory. The experimental points in the high η range appear to be systematically higher than would be expected.

The value of the quantity $c_0(-\Delta H)D_{\text{eff}}/\lambda\, T_0$ is about 0.01 for the catalyst used. Curves giving the effect of this variable (*28*) show that the error in η because of the temperature rise inside the catalyst pellet is less than 10%.

The estimated errors in the measurement of the reaction temperature and the product composition and flow rate lead to an estimated maximum error in the effectiveness factor of about 35%. A number of measurements were replicated, and the precision of the rate data seems to be in the order of 10%.

Figure 11 shows an Arrhenius plot of the results for the two catalyst sizes. The activation energy for the particles is 29.9 kcal./g. mole, in agreement with Natta's value (*1*). The points were calculated by Equation (1), and they describe a good straight line. The points for the pellets, which correspond to Equation (2), do not fall on a smooth curve. A line through the three points at the highest temperatures would have a slope of about one half the activation energy, so that it may be reasonable to think that the pellet rates at lower temperatures are high, as Figure 10 also shows.

Diffusion measurements have been made by Satterfield and Cadle at ambient conditions (*50*) and also at pressures to about 65 bars (*51*). These investigators found values of τ of 7.2 and 6.9 in the two studies cited. The surface area reported by Satterfield and Cadle is 44 sq.m./g.; for the catalyst used in the present study it is 130 sq.m./g. Otherwise, the properties of the two catalysts appear to be the same.

ACKNOWLEDGMENT

The generous support of a NASA fellowship and NSF Grant GK1918 are gratefully acknowledged. The University of Connecticut Computer Center is in part supported by NSF Grant GJ-9.

NOTATION

A = parameter in Equation (1)
B = parameter in Equation (1)
C = parameter in Equation (1)
c = concentration of carbon monoxide, g. mole/cc.
c_{eq} = concentration of carbon monoxide at equilibruim
c_0 = concentration of carbon monoxide at pellet surface
c_L = concentration of carbon monoxide at the center of the pellet
D = parameter in Equation (1)
D_{eff} = effective diffusivity, sq.cm./sec.
D_c = diffusivity of carbon monoxide through gas mixture, sq.cm./sec.
D_0 = diameter of pellet, cm.
D_{ij} = binary diffusion coefficient, sq.cm./sec.
f_i = fugacity of i, atm.
ΔH = heat of reaction, cal./g. mole
k = reaction rate constant
K = equilibrium constant
m = modulus defined by Equation (5)
p = total pressure, atm.
n = exponent in Equation (2)
r = reaction rate, g. mole/(g. catalyst)(hr.)
r_0 = reaction rate at pellet surface
T_0 = temperature at pellet surface, °K.
x_i = mole fraction of i

Greek Letters

α = dummy variable
β = dummy variable
ϵ = porosity of pellet
η = effectiveness factor
λ = thermal conductivity of pellet, cal.(cm.)/(sec.) °K.
τ = tortuosity

Subscripts

c = carbon monoxide
h = hydrogen
m = methanol

LITERATURE CITED

1. Natta, G., "Catalysis," Vol. 3, p. 349, P. H. Emmett, ed., Reinhold, New York (1955).
2. Capelli, A., and M. Dente, *Chim. e. Ind.*, **47**, 1068 (1965).
3. Uchida, H., and Y. Ogino, *Bull. Chem. Soc. Japan*, **31**, 45 (1958).
4. Ogino, Y., M. Oba, and H. Uchida, *ibid.*, **32**, 284 (1959).
5. *Ibid.*, 616.
6. *Ibid.*, **33**, 358 (1960).
7. Uchida, H., Y. Ogino, M. Oba, and K. Shimorura, *ibid.*, **35**, 1400 (1962).
8. *Ibid.*, 1638.
9. Temkin, M., and V. Pyzhev, *Acta Physicochim U.S.S.R.*, **12**, 327 (1940).
10. Tsuchiya, S., and T. Shiba, *J. Catal.*, **4**, 116 (1965).
11. Vlosenko, V. M., M. G. Rozenfel'd, and M. T. Rusov, *Intern. Chem. Eng.*, **5**, 195 (1965).
12. Münzing, E., *Chem. Technik*, **17**, 460 (1965).
13. Vachez, F., and P. Leprince, *Revue Inst. Francais Petrole*, **18**, 697 (1963).
14. Pasquon, I., and M. Dente, *J. Catal.*, **1**, 508 (1962).
15. Ellwood, P., *Chem. Eng.*, **12**, 104 (1968).
16. Carberry, J. J., *Ind. Eng. Chem.*, **56**, No. 11, 39 (1964).
17. Tajbl, D. G., J. B. Simons, and J. J. Carberry, *Ind. Eng. Chem. Fundamentals*, **5**, 171 (1966).
18. Brisk, M. L., R. L. Day, M. Jones, and J. B. Warren, *Trans. Inst. Chem. Engrs.*, **46**, T3 (1968).
19. Garanin, V. I., U. M. Kurkchi, and Kh. M. Minachev, *Kinetics and Catalysis*, **8**, 605 (1967).
20. Korneichuk, G. P., V. G. Vapichenko, and N. A. Konstantinova, *Kinetika Kataliz*, **7**, 358 (1966).
21. Korneichuk, G. P., *ibid.*, **4**, 518 (1962).
22. ———, and Yu. I. Pyatnitskii, *ibid.*, 157 (1962).
23. Korneichuk, G. P., and M. Ya. Rubanik, *ibid.*, **4**, 633 (1961).

24. Fulton, J. W., and O. K. Crosser, *AIChE J.*, **11**, 513 (1965).
25. Gioia, F., *Chim. e. Ind.*, **48**, 237 (1966).
26. Hutchings, John, and J. J. Carberry, *AIChE J.*, **12**, 20 (1966).
27. Chambers, R. P., and M. Boudart, *J. Catal.*, **6**, 141 (1966).
28. Satterfield, C. N., and T. K. Sherwood, "The Role of Diffusion in Catalysis," Addison-Wesley, Reading, Mass. (1963).
29. Raja Rao, M., N. Wakao, and J. M. Smith, *Ind. Eng. Chem. Fundamentals*, **2**, 127 (1964).
30. Moravec, P., P. Schneider, and M. Kraus, *Coll. Czech. Chem. Comm.*, **30**, 2908 (1965).
31. Beinert, R., and D. Gelbin, *Chem. Technik*, **19**, 207 (1967).
32. Otani, S., and J. M. Smith, *J. Catal.*, **5**, 332 (1966).
33. Cunningham, R. A., J. J. Carberry, and M. M. Smith, *AIChE J.*, **11**, 636 (1965).
34. Alcorn, W. R., D. Sc. thesis, Mass. Inst. Technol., Cambridge (1965).
35. Shabaker, R. H., Ph.D. thesis, Univ. Wisc., Madison (1965).
36. Wurzbacher, G., *J. Catal.*, **5**, 476 (1966).
37. Irving, J. P., and J. B. Butt, *Chem. Eng. Sci.*, **22**, 1859 (1967).
38. Miller, F. W., and H. A. Deans, *AIChE J.*, **13**, 45 (1967).
39. Brown, C. E., Ph.D. thesis, Univ. Conn., Storrs (1969).
40. Eckert, C. A., *Ind. Eng. Chem.*, **59**, No. 9, 20 (1967).
41. ———, and M. Boudart, *Chem. Eng. Sci.*, **18**, 174 (1963).
42. Bird, R. B., W. F. Stewart, and E. N. Lightfoot, "Transport Phenomena," Wiley, New York (1960).
43. Fuller, E. N., P. D. Schettler, and J. C. Giddings, *Ind. Eng. Chem.*, **58**, No. 5, 19 (1966).
44. Paratella, A., and I. Sorgato, "Proceedings Fourth International Congress on Catalysis," Novosibirsk (July 5-7, 1968).
45. Slattery, J. C., and R. B. Bird, *AIChE J.*, **2**, 137 (1958).
46. Lennert, D. A., and George Thodos, *Ind. Eng. Chem. Fundamentals*, **4**, 139 (1965).
47. Stiel, L. I., and George Thodos, *Can. J. Chem. Eng.*, **43**, 186 (1965).
48. Bischoff, K. B., *AIChE J.*, **11**, 351 (1965).
49. Aris, Rutherford, *Chem. Eng. Sci.*, **6**, 262 (1957).
50. Satterfield, C. N., and P. J. Cadle, *Ind. Eng. Chem. Proc. Design Develop.*, **7**, 256 (1968).
51. ———————, *Ind. Eng. Chem. Fundamentals*, **7**, 202 (1968).

Manuscript received November 18, 1968; revision received March 12, 1969; paper accepted March 14, 1969. Paper presented at AIChE New Orleans meeting.

Rate of Coalescence of the Dispersed Phase in a Laboratory Mixer Settler Unit: Part I

G. V. JEFFREYS, G. A. DAVIES, and K. PITT

The University of Aston in Birmingham, England

The rate of coalescence of large swarms of drops of a dispersed phase in the settler of a stage, laboratory mixer settler has been studied in order to establish the parameters that determine the dimensions of settlers used in extraction processes and effluent treatment. Part I is devoted to a description of the apparatus, experimental technique, and presentation of experimental results. Part II describes the development of a mathematical model which has been employed to analyze the results and is submitted as the basis for the design of settlers.

One of the most popular devices for contacting immiscible liquids in order to promote mass transfer is the mixer settler unit. This is due to its simplicity, ease of construction and operation, and the fact that high efficiencies can be expected irrespective of the characteristics of the liquids being treated. Thus, the mixer settler extractor may be considered in solvent extraction to be analogous to the bubble cap column in distillation. However, the performance of bubble cap distillation columns can be predicted fairly accurately, whereas techniques for the design or analysis of mixer settler extractors are nonexistent. Therefore, since these extractors are still being extensively employed in industrial applications, there is a need to establish criteria by which this equipment can be designed and analyzed.

A mixer settler extraction unit consists essentially of a number of stages, each of which contains a mixing chamber and a settling chamber. The mixer is usually provided with a propellor or turbine agitator and baffles, although in some, mixing is accomplished by means of a centrifugal pump. The emulsion generated in the mixer passes into the settling chamber through the mixed phase port and is distributed in the form of a wedge between the two phases in the settler. The dispersion wedge may exist above the interface if the more dense liquid is the dispersed phase, or below the interface if the less dense liquid is dispersed as illustrated in Figure 1. Settler operation is usually based on the principle that the emulsion wedge should not extend over the entire area of the interface, so that changes in throughput can be reflected in wedge length. If the wedge extends over the entire interface, increase in throughput must lead to an increase in the thickness of the wedge, with the result that raffinate tends to be lost through the extract port, and extract tends to pass through the raffinate port so that the efficiency of the unit is impaired. The problem of settler design is therefore an assessment of the factors that control the size of the emulsion wedge.

G. A. Davies and K. Pitt are at the University of Manchester, England.